Bulletin of the Seismological Society of America, Vol. 78, No. 2, pp. 617–635, April 1988

THE 1918 AND 1957 VANCOUVER ISLAND EARTHQUAKES

By John F. Cassidy, Robert M. Ellis, and Garry C. Rogers

Abstract

Since 1918, six significant earthquakes (5.2 < M < 7.2) have occurred in the region of central Vancouver Island where the Juan de Fuca, Explorer, and America plates interact. In this study, two of the largest earthquakes are examined in detail: the 1918 ($M_S \simeq 7$) and the 1957 ($M_S \simeq 6$) events.

The preferred location of the 1918 earthquake is on Vancouver Island at 49.44°N, 126.22°W, with a focal depth of 15 km. Magnitudes determined are M_S = 6.9 ± 0.3 and m_b = 7.2 ± 0.4. Analysis of surface waves suggests this is a predominantly strike-slip earthquake occurring along either a NNW- or an ENE-striking fault. The seismic moment is estimated as 7.40 × 10^{25} dyne-cm and the stress drop to be 122 bars.

The 1957 earthquake has been relocated on the continental shelf west of Vancouver Island at 49.64°N, 127.00°W, with a focal depth of 30 km. Magnitudes determined are M_S = 5.9 ± 0.2 and m_b = 6.3 ± 0.3. Surface wave and P-nodal analyses indicate that this is a predominantly strike-slip earthquake; either dextral along an NNW-striking fault, or sinistral along a ENE-striking fault. The seismic moment is estimated as 8.14 × 10^{24} dyne-cm and the stress drop to be 36 bars.

The 1918 earthquake appears to be a crustal intraplate event occurring in the lithosphere of the America plate, resulting from the complicated interaction of the Explorer, Juan de Fuca, and America plates. The preferred epicenter, depth, focal mechanism, and stress drop for the 1957 earthquake are consistent with the left-lateral motion between the Juan de Fuca and Explorer plates along the subducted extension of the Nootka fault zone. This earthquake is identical, within uncertainties, to events occurring in 1972 and 1986. We believe that these three earthquakes provide the best definition to date of both the position of the subducting portion of the Nootka fault zone west of Vancouver Island and the direction of relative motion along this fault.

Introduction

Since 1918, central Vancouver Island has experienced six significant (M = 5.2 to 7.2) earthquakes. This paper examines in detail the 6 December 1918 ($M \simeq 7$) and 16 December 1957 ($M \simeq 6$) earthquakes, two of the largest events.

The tectonic setting for these earthquakes is complex. West of Vancouver Island, the oceanic Juan de Fuca and Explorer plates lie between the major Pacific and America lithospheric plates and are being subducted beneath North America (Figure 1). Present-day convergence is estimated to be approximately 4 cm/yr in a northeasterly direction for the Juan de Fuca plate and less then 2 cm/yr in a more northerly direction for the Explorer plate (Riddihough, 1977, 1984). It is in the region where the projection of the Nootka fault zone (Hyndman *et al.*, 1979), which separates these two oceanic plates, intersects Vancouver Island that the six earthquakes have occurred. These events all have mechanisms which are predominantly strike-slip, with a similar orientation of nodal planes. Motion is either dextral on NW-striking planes or sinistral on NE-striking planes. Although these earthquakes have occurred near the projection of the Nootka fault zone, it is not obvious how or if they are all related to it. Rogers (1979) addressed this problem in an initial study of five of the events. Our detailed look at the 1918 and 1957 earthquakes and a preliminary

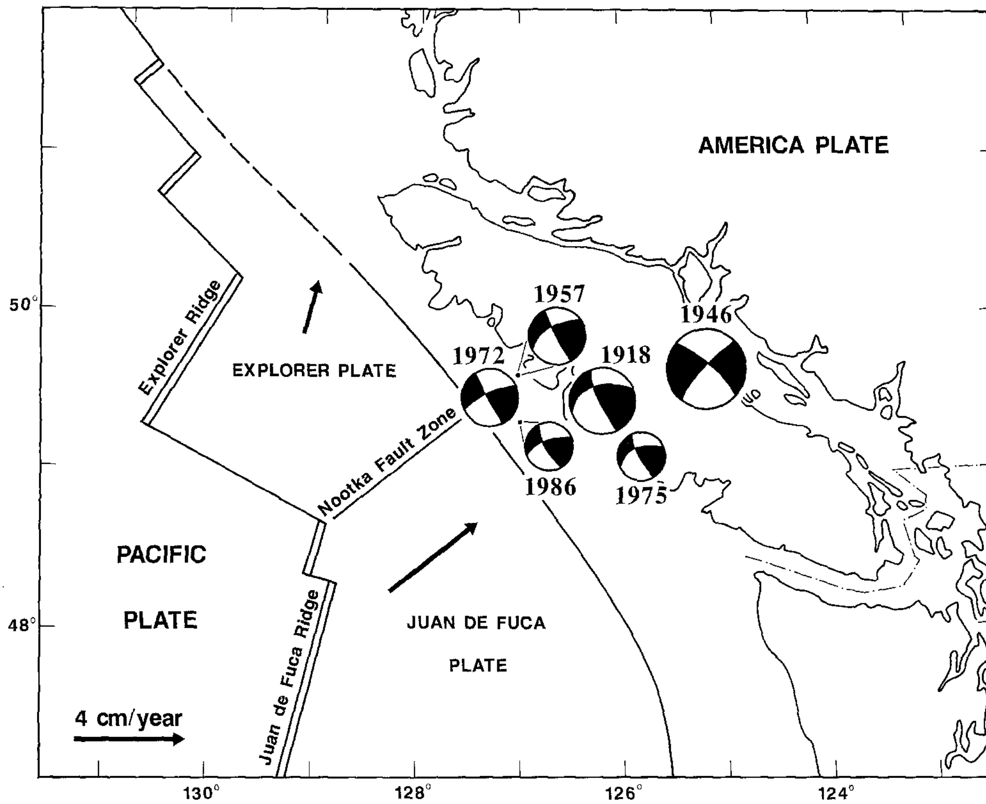

FIG. 1. The tectonic setting west of Vancouver Island. The lower hemisphere projections of the focal sphere represent the location of the largest earthquakes in this region. Circle radius is proportional to magnitude. The 1986 earthquake represents $M_L = 5.2$ and the 1946 earthquake represents $M_S = 7.2$. Mechanism solutions are from this paper and Rogers (1979).

analysis of the mechanism of the June 1986 event allows further understanding. For the two largest earthquakes, we investigate and redetermine the epicenters, estimate focal depths, determine well-constrained magnitudes, search for aftershocks, and thoroughly investigate the focal mechanisms.

Data Collection and Analysis Techniques

Seismograms for these earthquakes were obtained by making requests to stations which were known to be operating relatively long-period instruments in 1918 and 1957. In addition, seismograms and station bulletins for both earthquakes were purchased from the World Data Centre A–Historical Seismogram Filming Project. In total, 46 seismograms from 24 stations worldwide were obtained for the 1918 earthquake, and 138 seismograms from 46 stations were obtained for the 1957 earthquake.

Earthquake location. Teleseismic epicenters were calculated with a modified version of EPDET, an iterative least-squares program (Weichert and Newton, 1970) which uses the first arriving phases only. Stations having travel-time residuals greater than 60 sec were first rejected, then stations were successively culled at three different rejections levels. Typically, residual cut-offs of 10.0, 6.0, and 4.0 sec were used. Earth models considered were Jeffreys-Bullen (1958), Herrin (1968), and Dziewonski and Anderson (1981). Station corrections applied were those of Veith

(1975) associated with the Herrin (1968) model and Dziewonski and Anderson (1983) associated with their model. Our tests indicated that the Dziewonski and Anderson (1981) earth model with Dziewonski and Anderson (1983) station corrections provide the smallest travel-time residuals for each earthquake. This model with station corrections was used for final calculations.

The program HYPOELLIPSE (Lahr, 1984) was applied to determine hypocenters using the "local" technique. This program uses both P and S phases, and allows weights to be assigned to each arrival. The Vancouver Island-Puget Sound earth model (Rogers, 1983) was used.

Magnitude determination. Magnitudes determined are: m_b, according to the definition of Gutenberg and Richter (1956); M_S, according to the surface-wave magnitude of Vaněk *et al.* (1962); and a felt area estimate using the relationship of Toppozada (1975). This last relation, developed for crustal earthquakes in California and Nevada, relates total felt area to the original Richter local magnitude M_L and appears to be accurate to within ±¼ magnitude unit for earthquakes in the Vancouver Island region (Rogers, 1983).

Both vertical and horizontal components were used in magnitude determinations, with vector addition being applied to form total horizontal amplitudes from the N-S and E-W components.

Focal mechanism studies. Focal mechanism estimates were made using both the P-nodal technique and the radiation pattern of surface waves. A modified version of the program of Wickens and Hodgson (1967) was used for P-nodal analyses. The extended distance tables used in this program were those of Hodgson and Storey (1953) and Hodgson and Allen (1954a, b). Following the analysis of Rogers (1979), arrivals are assumed to be P_n at epicentral distances less than 20° and the take-off angle fixed at 60° for a crustal earthquake. While it is not clear that this is the case for the 1957 earthquake, restricting the take-off angle has little effect on a predominantly strike-slip mechanism.

The surface-wave method is based on the sensitivity of Rayleigh and Love wave amplitudes to the source mechanism, focal depth, and seismic moment. In these analyses, a point source is assumed with a step source-time function. The programs of Herrmann (1978) were used to determine spectral amplitudes of both Rayleigh and Love waves at all available stations. Amplitudes were corrected for instrument response and anelastic attenuation [the worldwide-averaged values of Tsai and Aki (1970) were applied] and were normalized to a reference distance of 9° (1,000 km). Typically, data from periods of 10 to 50 sec were useful for analysis. An algorithm (Herrmann, 1978) was then applied to determine the focal mechanism, depth, and seismic moment which provides the best fit to the data. The most important parameters which determine goodness of fit are the correlation coefficient between the observed and theoretical amplitude spectra at all azimuths and periods, for both Rayleigh and Love waves, and the agreement between the independent seismic moment estimates from Rayleigh and Love waves. Data and further details of analysis techniques may be found in Cassidy (1986).

THE 16 DECEMBER 1957 EARTHQUAKE—RESULTS

Intensity. On 16 December 1957 at 1727 UTC (09 27 local time), an earthquake was felt throughout central Vancouver Island (Figure 2). Newspapers from both the island and the adjacent mainland coast were searched for local reports of this earthquake. No damage was reported, and all newspaper reports are indicative of

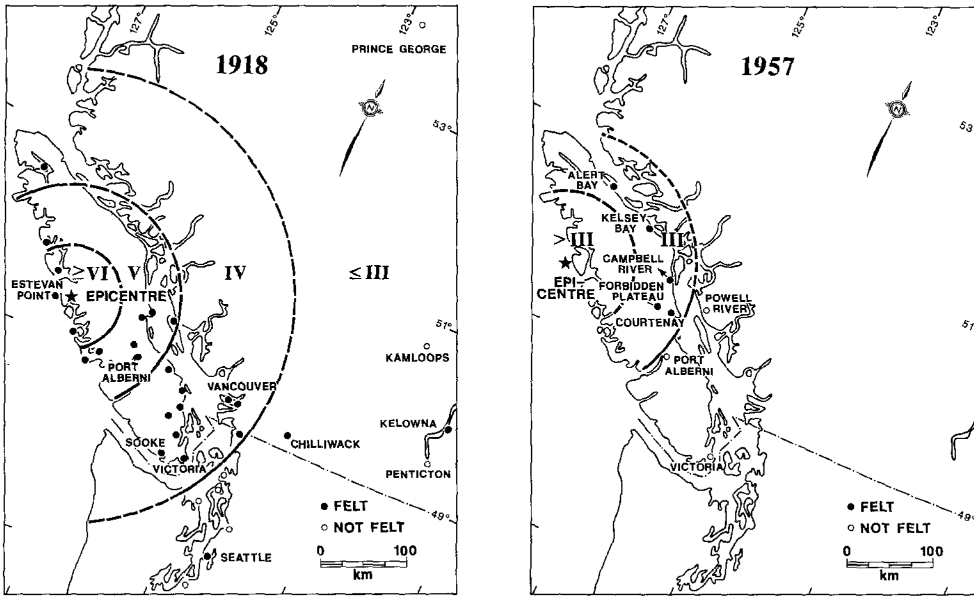

FIG. 2. Isoseismal maps for the 1957 (*right*) and 1918 (*left*) earthquakes. Solid lines indicate regions where the isoseismal boundaries are better constrained.

intensity III on the Modified Mercalli scale. It should be noted that there are no indications of this earthquake being felt in either Powell River or Port Alberni; this provides eastern and southeastern limits on the maximum felt area (88,900 km^2).

Epicenter. The epicenter was examined by considering teleseismic data, local data, and felt information. Previous epicenter estimates are shown in Figure 3 and listed in Table 1. A solution near that of Tobin and Sykes (1968) was obtained using their focal depth estimate of 0 km, the Jeffreys-Bullen earth model (which they applied), and the 100 P arrival times listed in the *International Seismological Summary* and the *Bulletin of the Bureau Central International Seismologie*. The Dziewonski and Anderson (1981) earth model was used for the remainder of the calculations. The complete teleseismic data set consisted of 113 P-wave arrival times, of which 34 were read directly from seismograms, 76 were obtained from the above-mentioned bulletins, and 3 were obtained from the unpublished worksheets of Milne.

Initial studies used the 113 arrival times with various focal depths. Travel-time residuals were found to be insensitive to depth over the range of 0 to 60 km. However, our surface-wave analysis indicated a focal depth near 30 km, and this value was used in subsequent calculations. A series of tests were conducted using various subsets of the data: only those stations having station corrections; neglecting those stations having large (>2.0 sec) residuals (it is more likely that a "late pick" would be made as opposed to an "early pick"); only those stations with impulsive arrivals; and only those stations both at epicentral distances greater than 20° and having station corrections. Of these tests, the latter, which reduces the effect of crustal and upper mantle structure on travel times, provided the best fit to the data. The solution obtained (Figure 3) of 49.64°N, 127.00°W with an origin time of 17 27 53.0 used 50 stations. This epicenter is offshore on the continental shelf, significantly SW of previous teleseismic epicenter estimates, all of which are on

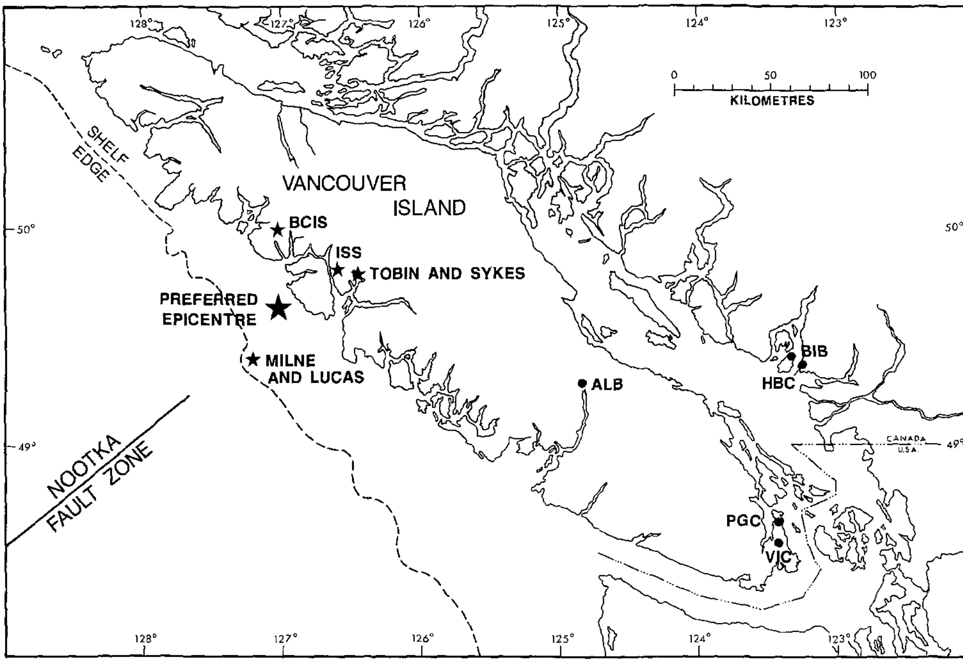

FIG. 3. Preferred epicenter for the 16 December 1957 earthquake and the previous estimates of the *International Seismological Summary (ISS) 1957 Bulletin, The Bureau Central International Seismologique 1957 Bulletin (BCIS)*, Tobin and Sykes (1968), and Milne and Lucas (1961). Also indicated are stations used to estimate a local epicenter and those stations (BIB and PGC) used to estimate station corrections for HBC and VIC.

TABLE 1

HYPOCENTRAL PARAMETERS FOR THE 1918, 1957, AND 1986 EARTHQUAKES

Event	Latitude (°N)	Longitude (°W)	Depth (km)	Origin Time (hh mm ss)	m_b	M_S	M	Reference
1918	49.0	124.0	—	08 41 03	—	—	—	ISS
	49.5	127.33	—	08 40 57	—	—	—	Denison (1919)
	49.75	126.5	<60	08 41 05	—	7.0	—	Gutenberg and Richter (1954)
	—	—	—	—	7.1	6.8	—	Abe (1981)
	49.62	125.92	—	08 41 05.8	—	—	7.0*	Rogers (1983)
	49.44	126.22	15	08 41 08.4	7.2	6.9	—	This study
1957	49.82	126.59	12	17 27 51	—	—	—	ISS
	50	127	—	17 27 47	—	6	—	BCIS
	49.82	126.48	0	17 27 48.7	—	—	—	Tobin and Sykes (1968)
	49.4	127.2	—	17 27 46.9	—	—	—	Milne and Lucas (1961)
	49.64	127.00	30	17 27 53.0	6.3	5.9	—	This study
1986	49.390	127.070	31	15 54 38.0	4.9	5.0	—	U.S. Geological Survey
	49.431	127.017	35.2	15 54 37.0	—	—	5.2†	Geological Survey of Canada

The abbreviations used are: ISS = International Seismological Summary; BCIS = Bureau Central International Seismologie.

* Felt area.

† M_L.

Vancouver Island. One concern is the azimuthal distribution of stations, notably the lack of data from azimuths of 180° to 270°. The effect of this distribution was estimated by considering the 5 July 1972 earthquake which occurred in the same epicentral region and was recorded over a more complete azimuthal range. This event was located using all data worldwide and then with a data set which matched the distribution of stations used for the 1957 solution. The epicenter moved approximately 12 km NE. This test indicates that the limited azimuthal distribution of stations for the 1957 earthquake had only a slight effect on the solution and suggests that the epicenter may be 12 km further SW, giving us confidence that the earthquake is located offshore.

Arrival times from four local stations (HBC, ALB, VIC, and SEA) (Figure 3) were used to determine a local epicenter. Using a recent earthquake in the region (5 April 1984), we generated station corrections for stations HBC, VIC, and ALB. Corrections for HBC and VIC, which are now closed, were estimated by calculating travel-time residuals from the recent event for the nearby stations BIB and PGC (Figure 3), respectively.

Our experimentation with the local data and station corrections leads us to believe the best local solution is in the vicinity of the Milne and Lucas (1961) local solution (Figure 3), about 30 km SW of our preferred teleseismic epicenter. This again gives us confidence that the earthquake is on the continental shelf rather than on Vancouver Island and also suggests that the true epicenter may be SW of our preferred teleseismic epicenter. We cannot explain the difference between the local and teleseismic solutions except that our experimentation with local arrival times suggests there may be a timing error we cannot detect. For this reason, we prefer the teleseismic epicenter with the comment that there is some evidence from the local data and our calibration experiment with the 1972 earthquake that the true epicenter may be located to the SW. Our experimentation with the teleseismic data leads us to assign an uncertainty of about ±20 km to our preferred epicenter. It is noted that the felt area of this earthquake applied to the total felt area-magnitude relationship of Toppozada (1975) also supports an offshore epicenter.

Focal depth. A number of methods were considered to estimate the focal depth of this earthquake. An unsuccessful search was made for the depth-dependent phase *pP*. As described previously, travel-time residuals for the preferred epicenter were found to be insensitive to depth over the range of 0 to 60 km. Hypocenter programs using local data only produced focal depth estimates of 0 to 25 km, but with uncertainties of about ±20 km.

Adequate depth bounds could be extracted from the surface-wave radiation patterns, especially Rayleigh waves which are very sensitive to depth. The algorithm used to determine the focal mechanism was run at focal depths ranging from 0 to 60 km. At each depth, the top scoring mechanism obtained was very similar. However, the surface-wave correlation factor (the product of the Rayleigh and Love wave correlation coefficients between the observed and theoretical spectra for all data) varied considerably with depth (Figure 4). This diagram shows the good fit to the data over the depth range of 25 to 40 km, with a maximum correlation at a depth of 30 km. The bounds of 25 to 40 km on the depth must be considered a minimum error estimate, as the effect (on depth) of errors in the surface-wave data are difficult to estimate.

The lack of aftershocks for this event (only one above $M_L = 2.3$ was recorded) also suggests that this earthquake occurred at a depth greater than 20 km. Few aftershocks are observed for events deeper than about 20 km throughout the

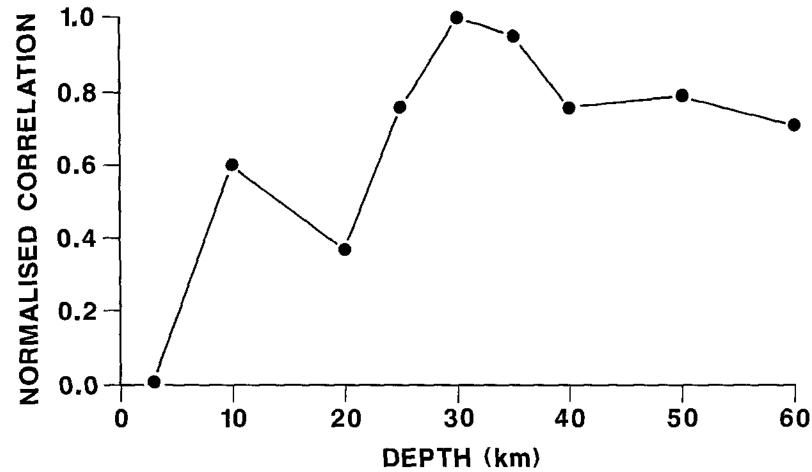

FIG. 4. Plot of normalized surface-wave correlation factor as a function of focal depth for the top scoring surface-wave solution of the 1957 earthquake. The best fit is at 30 km depth with bounds of 25 and 40 km.

Vancouver Island region. In a study of aftershock depths, Page (1968) determined that well-defined aftershock sequences only occur for shallow (<20 km) earthquakes. A focal depth of 30 km suggests that this earthquake occurred in the subducting plate.

Magnitude. The magnitudes determined for this earthquake using 22 stations are $m_b = 6.3 \pm 0.3$ and $M_S = 5.9 \pm 0.2$ where the uncertainties are one standard deviation. A magnitude estimate based on the total maximum felt area estimate of 88,900 km^2 is 5.7.

Source mechanism. A poorly constrained *P*-nodal mechanism (Rogers, 1979) suggests this event is predominantly strike-slip and similar to other events in the central Vancouver Island region. In this study, both the *P*-nodal technique and the radiation pattern of surface waves were used to estimate the source mechanism.

First-motion data were available from a total of 50 stations. In processing, clear arrivals with known instrument polarity were given full weight, and readings from bulletins, unclear arrivals, or instruments of uncertain polarity were given half-weight.

The results of the *P*-nodal analysis are illustrated in Figure 5a. The top scoring solution is very similar to that obtained by Rogers (1979). This was expected, as the only differences in the data sets are the addition of 12 first motions in this study and the reversal of the polarity (based on station bulletin information) of the first motion at Santa Clara, California (SCL). This station helped define the NW–SE-striking nodal plane in the solution of Rogers. Our revised solution is predominantly strike-slip, with a fault plane oriented either N74°E, dipping 71° in a northerly direction or N24°W, dipping 67° in a westerly direction. This mechanism is not well constrained due to a lack of data between azimuths of 180° and 300°. The take-off angles for those stations at epicentral distances (Δ) less than 20° are difficult to estimate due to the complicated geological structure of this subduction zone (e.g., Spence *et al.*, 1985). Several California stations ($\Delta \simeq 17°$) and two Alaska stations ($\Delta \simeq 9°$ and 19°) define the NNW-striking nodal plane of the preferred solution. The uncertainty in the take-off angles for these stations may be as much as ±15°. Although this may slightly change the orientation of the NNW-striking plane, it cannot change the mechanism significantly.

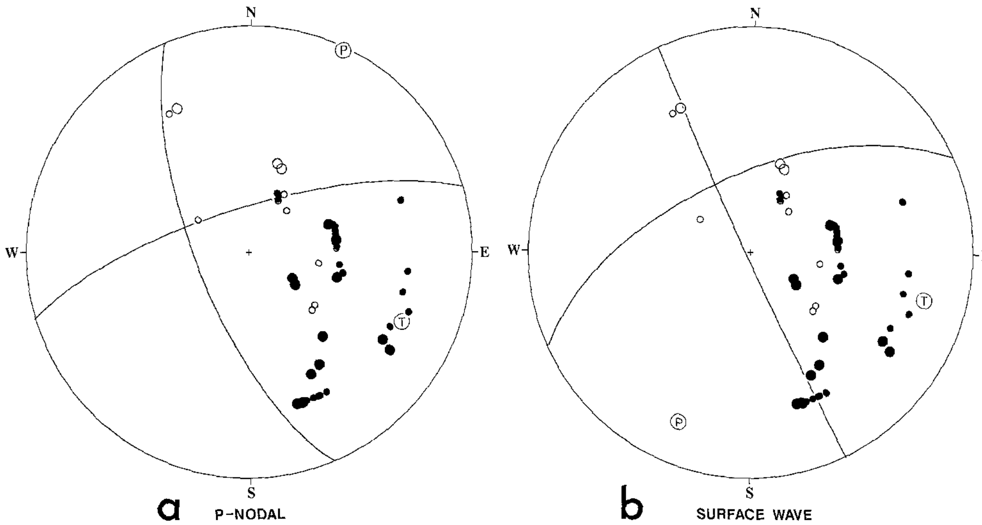

FIG. 5. Focal mechanisms for the 1957 earthquake as derived from P-nodal and surface-wave analyses. The lower half of the focal sphere is shown. In the case of the surface-wave solution, the first-motion data have been superimposed on the sphere. P and T represent pressure and tension axes, respectively. Dots indicate compressional arrivals, and open circles represent dilational arrivals. Smaller symbols are less reliable data given one-half weight in the processing (see text).

Possible mechanisms were further evaluated by analysis of surface waves recorded at 20 stations ranging in azimuth from 328° to 163°. The eight-layered earth model of Ben-Menahem and Singh (1981) and the 625 observed spectral amplitudes in the period range of 16 to 80 sec were used. The program was run with the focal depth being varied from 3 to 60 km. The best-fit mechanism, shown in Figure 5b with first motions superimposed, has nodal planes striking N65°E, dipping 62° in a northerly direction and N26°W, dipping 88° in a westerly direction. This mechanism provided a best fit to the data at a focal depth of 30 km. Nodal planes have been resolved to 4° and have a total uncertainty of about ±10°. This solution is very similar to the best-fit solution obtained by the P-nodal technique. There are several stations which have first motions in agreement with the P-nodal solution, but are inconsistent with the surface-wave solution. The majority of these stations, however, are close to a nodal plane, and within uncertainty of the surface-wave analysis and take-off angle estimates are in agreement with the solution.

Theoretical radiation patterns for Rayleigh and Love waves for the best-fit surface wave mechanism at 30 km depth are shown in Figure 6, with observed data corrected for anelastic attenuation and normalized to a reference distance of 1,000 km. There is considerable scatter, particularly for Rayleigh waves; however, the stations which deviate the most from the theoretical radiation patterns are those which either have the largest uncertainties in calibration data or for which the surface waves have a mixed (continental-oceanic) travel path. Considering the uncertainties in the magnification of most of the instruments, the mixed travel paths which the surface waves have traversed, and the uncertainty in attenuation values, these data provide an adequate fit to the theoretical radiation patterns.

As a further check of possible mechanism solutions, the theoretical surface-wave radiation patterns of alternate but lower scoring P-nodal solutions were generated. In all of the cases, the theoretical pattern was in poor agreement with the observed surface-wave amplitude data.

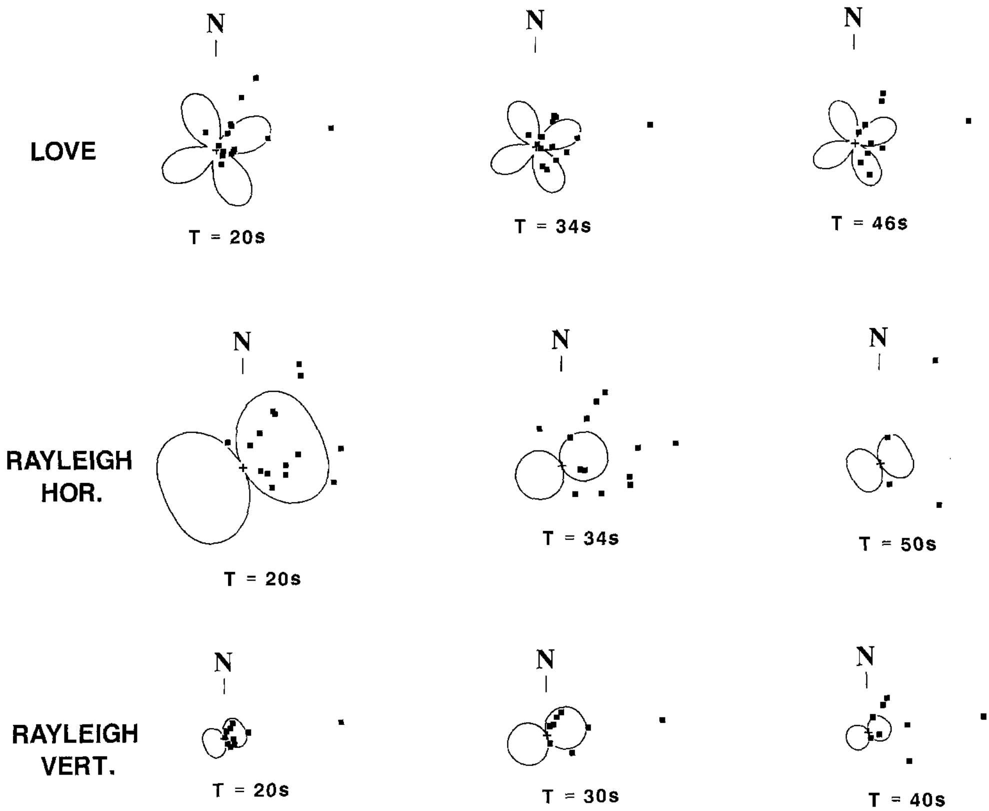

FIG. 6. Observed (dots) and theoretical (solid lines) Love wave (*top*), horizontal Rayleigh wave (*middle*), and vertical Rayleigh wave (*bottom*) radiation patterns at selected periods for the best-fit surface-wave solution of the 1957 earthquake (Figure 5) at a focal depth of 30 km. Each dot represents the spectral amplitude at a station. The azimuth of the dot represents the station azimuth, and the distance from the center of the pattern is proportional to the spectral amplitude (normalized to a reference distance of 1,000 km). The wave period is given *below* each pattern.

In summary, the best-fit surface-wave mechanism is similar to the best-fit *P*-nodal solution and is predominantly strike-slip. The surface-wave solution is the preferred mechanism based on the fit it provides to both surface-wave data and first-motion data. The possibility that the slight differences between first-motion and surface-wave mechanism solutions are real cannot be ruled out, as the *P*-nodal solution represents the first rupture motion, and the surface-wave solution represents the average rupture motion which may be different.

Seismic moment, stress drop, and aftershocks. The seismic moment of this earthquake estimated from the amplitudes of surface waves is $M_0 = 8.14 \times 10^{24}$ dyne-cm. This estimate is subject to errors of up to 50 per cent, due to uncertainties in focal depth, attenuation values, and intrinsic errors in the surface-wave data.

Applying the Kanamori and Anderson (1975) relation between seismic moment and surface-wave magnitude results in a stress drop estimate of 36 bars for this earthquake. This is close to the stress drop of $\approx$30 bars they suggested for interplate earthquakes. Given the uncertainty of $\pm$50 per cent in the seismic moment estimate, and the uncertainty of $\pm$0.2 in M_S, stress drops ranging from 20 to 90 bars are possible.

This earthquake had only one recorded aftershock. It occurred on 17 December at 07 46 15.4 and was recorded at ALB only. Milne and Lucas (1961) estimated the magnitude to be $M_L = 2.8$. The lowest detectable magnitude at this time was $M_L = 2.3$ (Rogers, 1979).

THE 6 DECEMBER 1918 EARTHQUAKE—RESULTS

Intensity. On 6 December 1918 at 0841 UTC (00 41 local time), an earthquake was felt throughout Vancouver Island as well as in Vancouver and Seattle. Effects were also observable in the Okanagan valley community of Kelowna, approximately 470 km from the epicenter. Intensity data obtained from Denison (1919) and a thorough search of British Columbia and Washington state newspapers are shown in Figure 2.

Due to sparse population in the epicentral region, no injuries and little damage resulted. The earthquake was felt most severely at Estevan Point lighthouse where the steel reinforced concrete of the 33.5 m tower cracked its full length in several places and parts of the glass lens were smashed, temporarily rendering the lighthouse inoperable. Throughout central Vancouver Island, we assign intensity V based on numerous reports of windows rattling, pendulum clocks stopping, pictures and dishes falling to the floor, and some instances of cracked plaster. In Kelowna, several pendulum clocks stopped, several people heard a noise but felt no shaking, and one person felt a building on a wharf sway. There are no reports in newspapers of this earthquake being felt in other interior communities (Penticton, Kamloops, and Prince George), but this is likely due to the time of occurrence. The total felt area obtained by drawing a circle around the epicenter and limited in radius by Kelowna is approximately 690,000 km^2.

Epicenter. The epicenter of this event was examined using the teleseismic method. Previous epicenter estimates are shown in Figure 7 and listed in Table 1. Travel-time residuals and epicenter estimates were found to be insensitive to focal depth over the range of 0 to 30 km. A depth of 15 km based on surface-wave studies was used for the following calculations.

A total of 49 arrival times, of which 18 were measured from seismograms and 31 were obtained form the 1918 *International Seismological Summary Bulletin*, were used in this study. Picking accurate P-arrival times was difficult due to low-gain instruments, slow drum speeds (15 mm/min), nonuniform rotation rates, and uncertainties in timing. Using the entire data set resulted in an epicenter (21 stations in the solution) 12 km west of Roger's (1983) estimate. A series of tests were conducted using various subsets of the data including: neglecting those stations having travel-time residuals greater than 2.0 sec ("late picks"); using only those stations having station corrections; increasing the final travel-time residual rejection limit from 4.0 to 10.0 sec; and using only those stations both at distances greater than 20° and having station corrections. The last test described provided the best fit to the data, although only nine stations were included in the solution. The epicenter of 49.44°N, 126.22°W is 30 km southwest of Roger's (1983) epicenter estimate (see Figure 7). Clearly, there is a trade-off between the larger amount of data and fewer data of higher quality; we chose the latter. Other tests, those stations having Dziewonski and Anderson station corrections only and the data set having a 10.0 sec rejection limit, resulted in epicenters within 15 km of that previously described and included more stations in the solution, 14 and 29 respectively. A test of the azimuthal distribution of stations, as described for the 1957 earthquake, resulted in a movement of only 9 km NE due to the limited data set.

The solution of 49.44°N, 126.22°W and origin time 08 41 08.4 is preferred because the data set (only those travel-times with station corrections and not affected by

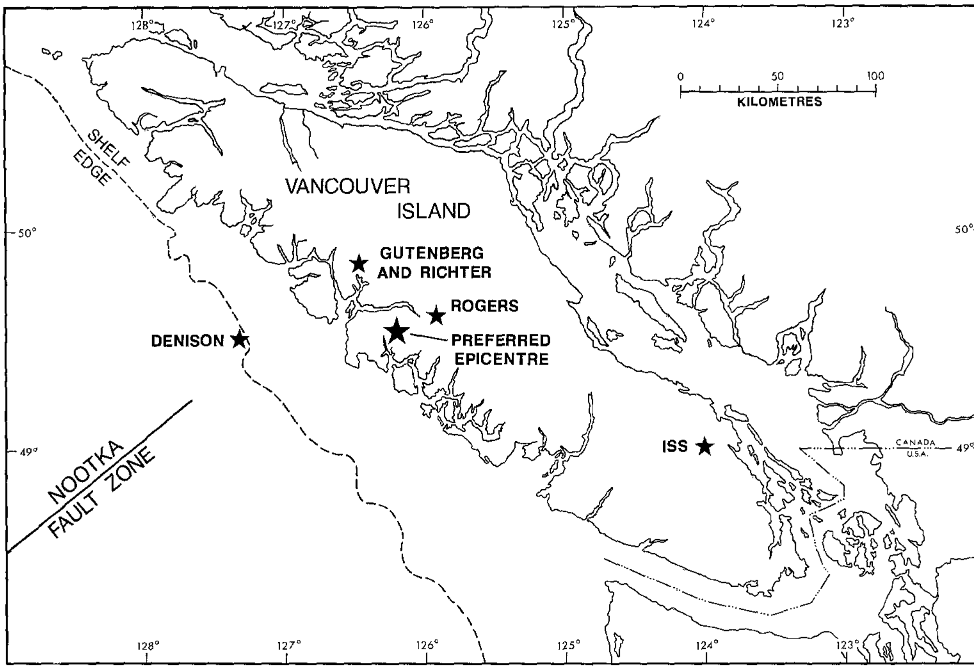

FIG. 7. Preferred epicenter for the 6 December 1918 earthquake and the estimates of Denison (1919), the *International Seismological Summary (ISS) 1918 Bulletin,* Gutenberg and Richter (1954), and Rogers (1983).

crustal or upper mantle structure) produced the smallest travel-time residuals. Similar data sets used for the 1957 and 1972 earthquakes produced both the smallest travel-time residuals and the best agreement with local epicenter solutions. Given the small number of stations in the solution, the possibility of azimuthal bias and the poor quality of data, we estimate an uncertainty of about ±30 km.

Focal depth. Body waves were not useful for estimating the depth of this earthquake. The phase *pP* could not be identified on any seismograms, and travel-time residuals were found to be insensitive to focal depth over the range of 0 to 30 km.

Again, the focal depth was estimated by comparing the observed radiation pattern of surface waves with theoretical patterns generated at various depths. The surface-wave correlation factor, as described previously, was calculated for the best-fit focal mechanism at depths of 5 to 50 km. Figure 8 shows a good fit at depths of 5 to 20 km and the maximum correlation at a depth of 15 km. Based on these data (Figure 8), the preferred focal depth is 15 km, with bounds of 5 and 20 km.

The large number of aftershocks (13 to 14) recorded for this event support a shallow focal depth (Page, 1968), which for an event of this size probably implies surface rupture.

Magnitude. Published magnitudes for this earthquake are given in Table 1. It is not known how many stations were used in these studies. Magnitude estimates from this study are $m_b = 7.2 \pm 0.4$ (18 stations) and $M_S = 6.9 \pm 0.3$ (20 stations). The felt area magnitude, based on a total felt area estimate of 690,000 km^2 (assuming a circular total felt area and Kelowna as the most distant felt report) is 7.0.

Source mechanism. The small data set and quality of the data set did not permit a *P*-nodal analysis. Only one station, Washington D.C. (WAS), had a clear arrival with both the component and polarity indicated on the seismograms.

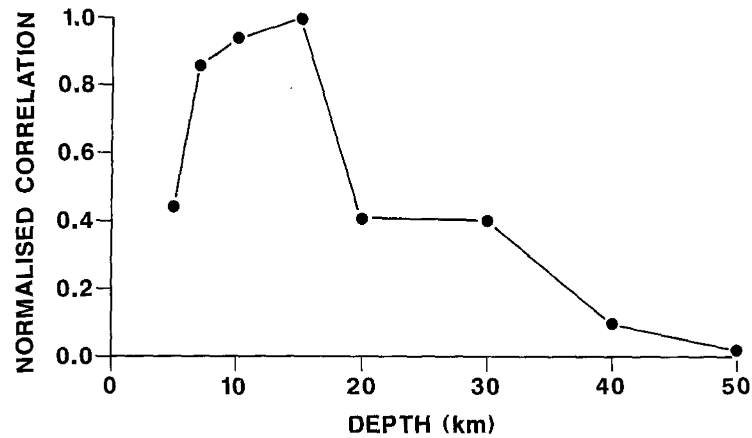

FIG. 8. Plot of normalized surface-wave correlation factor as a function of depth for the preferred mechanism of the 1918 earthquake. The best fit is obtained at a depth of 15 km; bounds are estimated to be 5 to 20 km.

Surface-wave analysis. Surface waves recorded at 10 stations with azimuths from 327° to 164° were available for analysis. Overall, the data are of poorer quality than those of the 1957 earthquake, with the major problem being uncertainty in instrument parameters. In addition, all but one of the stations had seismographs with pendulum periods less than 20 sec and therefore are not as sensitive to longer period waves which are more diagnostic. For a magnitude 7 earthquake, which may have a rupture length of up to 35 km (e.g., Acharya, 1979), the point source approximation beings to break down for waves having periods less than 20 to 30 sec. The critical period depends on the rupture velocity and orientation of the stations with respect to the fault (Tsai and Aki, 1970). This approximation must be considered another possible source of error in this analysis. A total of 232 Love, Rayleigh horizontal, and Rayleigh vertical spectral amplitudes over a period range of 14 to 56 sec were determined for the 10 stations. For such a small data set, the least-squares fitting routine was not appropriate. In this case "forward modeling" was attempted. The radiation patterns for mechanisms of other earthquakes in this region [1946, 1972, 1975 (see Figure 1), and the 1957 event (Figure 5)] were generated and compared to the observed data. In addition, the radiation patterns of thrust and normal mechanisms with a fault strike oriented parallel to the subduction zone (coastline) and dips ranging from 10° to 30° were generated and compared to the observed data. The thrust and normal mechanisms provide a poor fit to the observed data and rule out these types of solutions. The surface-wave radiation pattern of the 1975 mechanism of Rogers (1979) (see Figure 9) at a focal depth of 15 km and with a seismic moment of 0.74×10^{26} dyne-cm produced the best fit with the observed data. This solution, together with a clear compressional arrival at WAS, indicates either left-lateral predominantly strike-slip motion along a fault striking N77°E and dipping 48°NW, or predominantly right-lateral strike-slip motion with a large component of thrust along a fault striking N19°W and dipping 83°SW.

Figure 10 shows the observed and theoretical radiation patterns for this mechanism. The Love wave pattern provides a good fit to the data, and the Rayleigh wave pattern fits the nearly E-W lobe observed in the data, especially for periods near 18 to 24 sec where the surface-wave energy was best recorded. The stations which

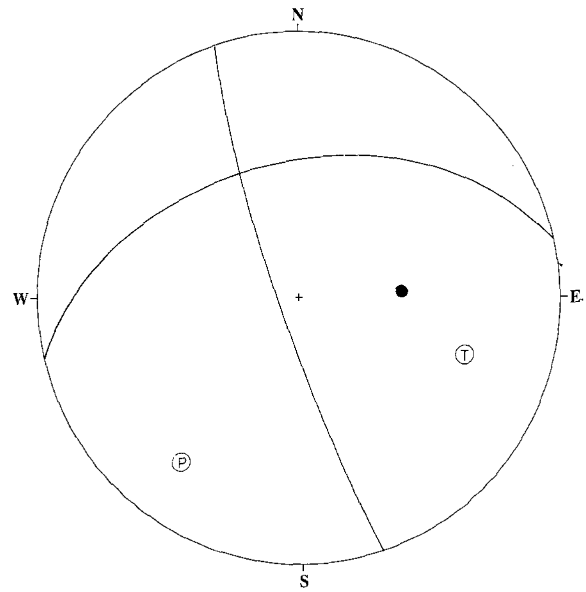

FIG. 9. Mechanism of the 1975 earthquake from Rogers (1979) (Figure 1) which provides a good fit to the observed surface-wave data for the 1918 event. A clear first arrival (WAS) in the center of the SE quadrant indicates that this is a compressional quadrant.

deviate the most from these patterns are again those stations (MHC and SIT) for which surface waves have propagated along the continental/oceanic boundary. The 1957 mechanism (Figure 5) provides only a slightly poorer fit to the surface-wave data than the 1975 mechanism and serves to illustrate that the solution for the 1918 earthquake is poorly constrained due to the small data set, uncertainties involved in instrument response, and mixed travel paths.

Seismic moment, stress drop, and aftershocks. The seismic moment for this earthquake, estimated from surface-wave amplitudes and assuming the 1975 mechanism at a focal depth of 15 km, is 0.74×10^{26} dyne-cm. Applying the relation of Kanamori and Anderson (1975) between seismic moment and magnitude results in a stress drop of 122 bars, consistent with an intraplate earthquake (>100 bars). This is not definitive, however; doubling the moment estimate (which is not unreasonable given the quality of the data) and considering the uncertainty of ± 0.3 in the surface-wave magnitude can result in stress drops as low as 30 bars (i.e., interplate).

This earthquake had 13 felt aftershocks. The largest occurred approximately 4 hr after the main shock and was felt throughout central Vancouver Island (Port Alberni, Estevan Point, and Courtenay). The others were much smaller and felt only at Estevan point (10 were felt the day after the main shock). For the largest aftershock, a felt area magnitude was estimated to be 5.1. This, however, is likely low, as the aftershock occurred at 0400 local time while most people were sleeping, and therefore the total felt area estimate is likely low. A record of this aftershock obtained from the European station DBN permitted a surface-wave magnitude determination. The estimate of $M_S = 5.9$ is probably high, as the main shock magnitude estimate at this station is 0.3 unit higher than the mean. We thus estimate the magnitude of the largest aftershock as 5.6.

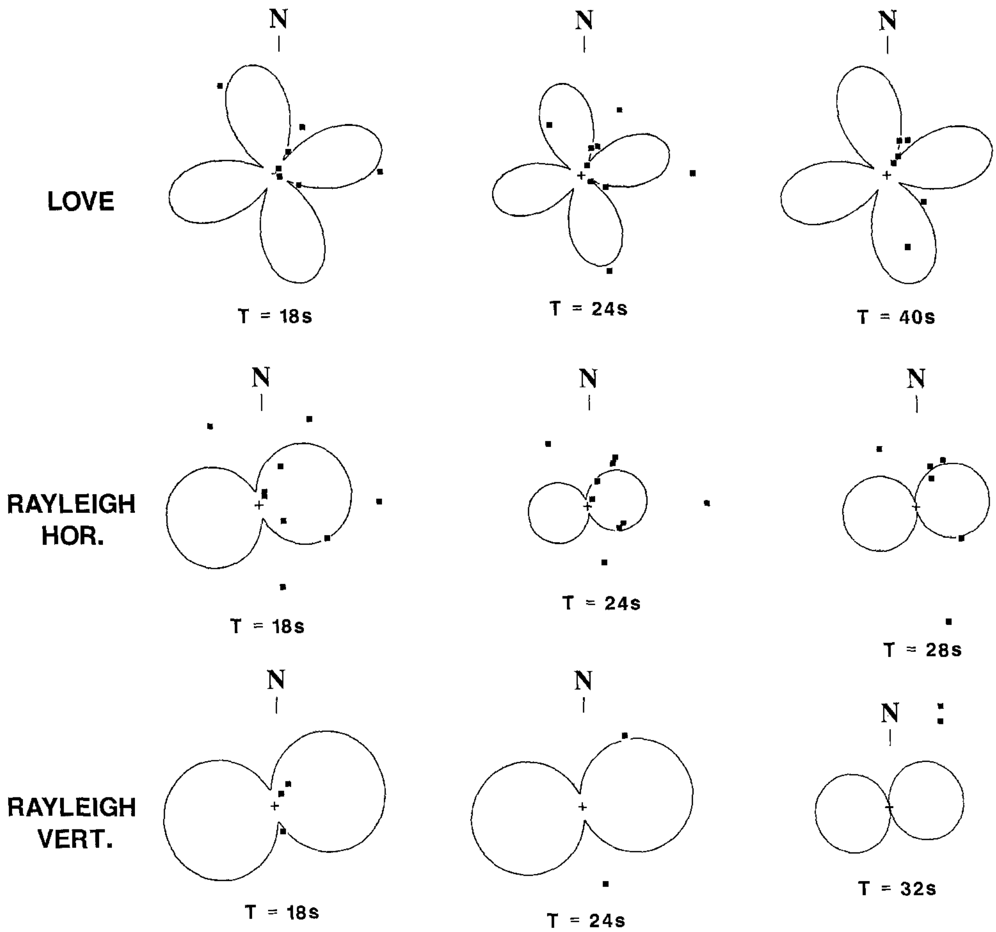

FIG. 10. Observed (dots) and theoretical (solid lines) Love wave (*top*), horizontal Rayleigh wave (*middle*), and vertical Rayleigh wave (*bottom*) radiation patterns for the best-fit surface-wave solution of the 1918 earthquake (Figure 9) at a focal depth of 15 km. (Notation the same as for Figure 6.)

THE 16 JUNE 1986 EARTHQUAKE

During our detailed study of the 1918 and 1957 earthquakes, an earthquake of $M_L = 5.2$ occurred at 15:54 on 16 June 1986 just offshore from central Vancouver Island. Preliminary solutions (Table 1) by the Canadian Geological Survey (National Summary) and the U.S. Geological Survey (Preliminary Determination of Epicenters) give it a location and depth very similar to the 1957 and 1972 earthquakes (Figure 1). Like the earlier events, its focal depth is about 30 km, and it had few aftershocks with the largest about magnitude 2. We have computed a preliminary P-nodal focal mechanism (Figure 11) using first motions read from seismograms of the Canadian network and the Alaska Tsunami Warning network and first motions published in the Earthquake Data Reports of the U.S. Geological Survey. The solution is similar to the 1957 and 1972 solutions and appears to be well-defined, but we consider it as preliminary until more data are examined first hand. However, the similarity of the three solutions gives us confidence that they are representative of fault motion in the area of the earthquakes.

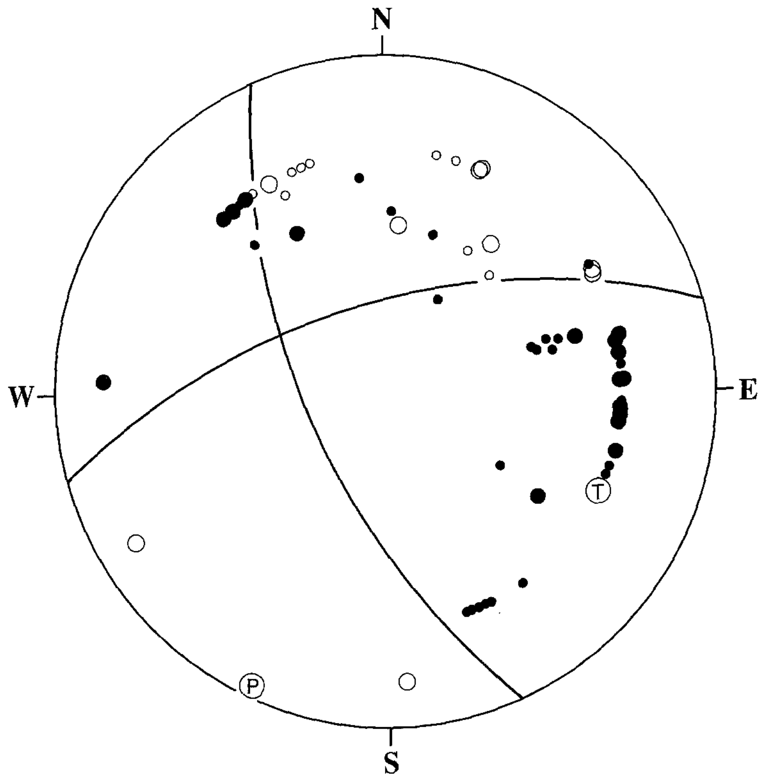

FIG. 11. Preliminary P-nodal solution of the 16 June 1986 earthquake. Presentation the same as in Figure 5.

SUMMARY AND CONCLUSIONS

Our results are summarized in Table 2. The preferred epicenter of the 1957 earthquake is ≈40 km SW of previous estimates by the International Seismological Summary and Tobin and Sykes (1968). This offshore solution is supported by both local data and felt information. The depth estimate of 30 km obtained from surface-wave studies suggests that this earthquake occurred in the upper portion of the subducting oceanic plate (see Figure 12). The focal mechanism of this earthquake determined by P-nodal and surface-wave analyses is similar. They suggest a predominantly strike-slip earthquake occurring along a fault striking approximately ENE or NNW. The preferred surface-wave solution (Figure 5) has a pressure axis near 200°, similar to those of other large events in this region (Rogers, 1979). Thrust or normal mechanisms which are often associated with subduction zones (e.g., Isacks *et al.*, 1968) are ruled out by this study for both the 1918 and 1957 earthquakes. For the 1957 earthquake, the possible left-lateral strike-slip focal mechanism along a fault striking approximately NE, depth in the upper portion of the subducting plate, and low stress drop indicative of an interplate earthquake are consistent with left-lateral slip between the Juan de Fuca and Explorer plates along the subducting Nootka fault zone.

The similarity of the 1957 earthquake to the 1972 (Rogers, 1976) and 1986 earthquakes should be noted. The location, depth, focal mechanism (see Figures 1 and 12), and aftershock pattern of these earthquakes are identical within uncertain-

TABLE 2
SUMMARY OF RESULTS

	1918 12 06	1957 12 16
Origin Time	08 41 08.4	17 27 53.0
Epicenter	49.44°N, 126.22°W (±30 km)	49.64°N, 127.00°W (±20 km)
Depth	15 km, bounds 5–20 km	30 km, bounds (25–40 km)
Magnitude	$M_S = 6.9 \pm 0.3$, $m_b = 7.2 \pm 0.4$	$M_S = 5.9 \pm 0.2$, $m_b = 6.3 \pm 0.3$
Mechanism	Predominantly strike-slip along either: Strike = N77°E Dip = 48°NW (left-lateral) Strike = N19°W Dip = 83°SW (right-lateral)	Predominantly strike-slip along either: Strike = N65°E Dip = 62°NNW (left-lateral) Strike = N26°W Dip = 88°SW (right-lateral)
P axis	Azimuth = 217°, Dip = 23°	Azimuth = 203°, Dip = 18°
T axis	Azimuth = 110°, Dip = 34°	Azimuth = 106°, Dip = 21°
M_0	7.40×10^{25} dyne-cm	8.14×10^{24} dyne-cm
Stress drop	122 bars	36 bars
Aftershocks	13 felt, the largest magnitude ≃5.6	Only one above $M_L = 2.3$, $M_L = 2.8$

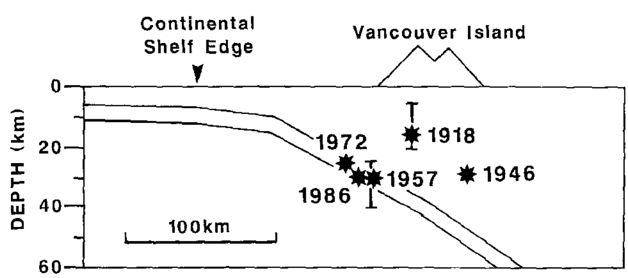

FIG. 12. Cross-section of the subduction zone near Vancouver Island with 2:1 vertical exaggeration. This diagram shows the depth of the 1918, 1946, 1957, 1972, and 1986 earthquakes in relation to the subducting plate. The depth estimate for the 1946 earthquake is from Rogers and Hasegawa (1978). *Error bars* for the 1918 and 1957 earthquakes are based on the surface-wave correlation factor and must be considered a minimum estimate of the uncertainty. The geometry of the subducting plate is based on Spence *et al.* (1985) and J. Drew (1987).

ties. Horizontal projections of slip vectors for each nodal plane of the three earthquakes are shown in Figure 13. The slip vectors determined for the 1986 earthquake are based on the preliminary P-nodal mechanism in Figure 11. Slip vectors are clustered in two groups, one oriented NNW and one oriented WSW. The NNW group coincides with the approximate orientation of the plate margin in this region. The WSW group is oriented in a slightly more southerly direction than the estimated Explorer-Juan de Fuca plate interaction 0.5 m.y. ago (Riddihough, 1977). These WSW slip vectors are preferred based on previous arguments of location, depth, focal mechanism, and stress drop consistent with movement along the Nootka fault. The WSW-oriented slip vectors are likely the best definition of contemporary motion along the subducting portion of the Nootka fault zone just west of Vancouver Island.

The epicenter we chose for the 1918 earthquake is about 30 km SW of the previous estimate of Rogers (1983). The depth estimate of 15 km from surface-wave analysis is supported by the large number of aftershocks observed for this event. This indicates that the earthquake occurred in the overlying continental lithosphere rather than in the subducting plate (see Figure 12). It is interesting to note that

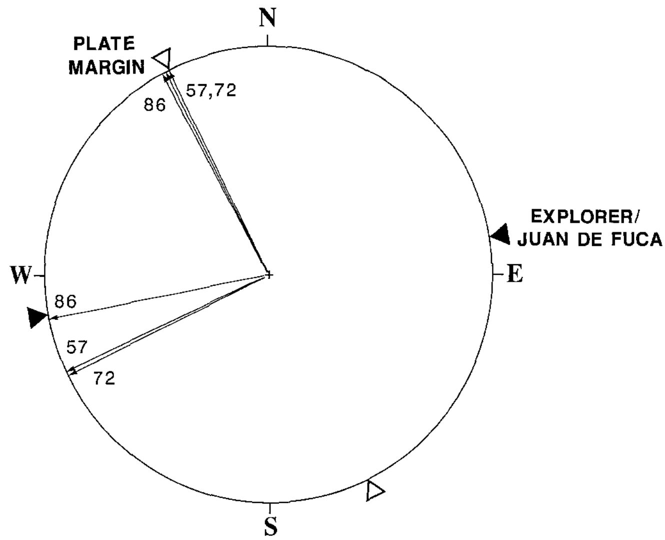

FIG. 13. Horizontal projection of the slip vectors on the two possible fault planes for the mechanisms of the 1957, 1972, and 1986 earthquakes. The 1972 slip vectors are revised from Rogers (1979). Large solid arrowheads indicate the orientation of the Explorer-Juan de Fuca plate interaction 0.5 m.y. ago from Riddihough (1977). Large open arrowheads indicate approximate orientation of the plate margin in this region.

there are inferred NNW-striking faults in the epicentral region (Muller *et al.*, 1980), in agreement with a NNW nodal plane for the preferred surface-wave solution. The poorly constrained mechanism appears to be predominantly strike-slip and similar to the mechanism of the 1975 earthquake, which occurred approximately 30 km SE (Figure 1). The large stress drop estimate of 122 bars suggests that this is an intraplate event in agreement with the shallow focal depth. The 1918 earthquake is different from the other significant events (1946, 1957, and 1972) in that it had a large number of aftershocks, including one that was relatively large ($M \simeq 5.6$). This again is supportive of a shallow focal depth. It is similar to the others in that it is predominantly strike-slip, and similar to the 1946 earthquake in that it occurred in the continental crust and further inland than the other events. The quality of the data used in this study do not allow for an unambiguous interpretation of this earthquake in terms of seismotectonic models. However, the location, focal depth, and stress drop suggest a crustal intraplate earthquake not directly associated with the Nootka fault zone. This earthquake is likely due to the stress regime in the continental crust which results from the coupling of the obliquely subducting Juan de Fuca and Explorer plates with the America plate.

ACKNOWLEDGMENTS

Financial support for this study was provided by Energy, Mines and Resources Canada Research Agreements 25/03/85 and 19/03/86 to the University of British Columbia.

REFERENCES

Abe, K. (1981). Magnitudes of large shallow earthquakes from 1904 to 1980, *Phys. Earth Planet. Interiors* **27,** 72–92.

Acharya, H. K. (1979). Regional variations in the rupture-length magnitude relationships and their dynamic significance, *Bull. Seism. Soc. Am.* **69,** 2063–2084.

Ben-Menahem, A. and S. J. Singh (1981). *Seismic Waves and Sources*, Springer-Verlag, New York, 1108 pp.

Cassidy, J. F. (1986). The 1918 and 1957 Vancouver Island Earthquakes, *M.S. Thesis*, University of British Columbia, Vancouver, British Columbia, 143 pp.

Denison, F. N. (1919). The British Columbia earthquake of December 6, 1918, *Bull. Seism. Soc. Am.* **9,** 20–23.

Drew, J. J. (1987). A re-evaluation of the seismic structure across the active subduction zone of western Canada, *M.S. Thesis*, University of British Columbia, Vancouver, British Columbia, 144 pp.

Dziewonski, A. M. and D. L. Anderson (1981). Preliminary reference Earth model, *Phys. Earth Planet. Interiors* **25,** 297–356.

Dziewonski, A. M. and D. L. Anderson (1983). Travel times and station corrections for *P* waves at teleseismic distances, *J. Geophys. Res.* **88,** 3295–3314.

Gutenberg, B. and C. F. Richter (1954). *Seismicity of the Earth and Associated Phenomena*, Princeton University Press, Princeton, New Jersey, 310 pp.

Gutenberg, B. and C. F. Richter (1956). Magnitudes and energy of earthquakes, *Ann. Geofis.* **9,** 1–15.

Herrin, E. (1968). Seismological tables for *P* phases, *Bull. Seism. Soc. Am.* **58,** 1193–1241.

Herrmann, R. B. (1978). *Computer Programs in Earthquake Seismology*, 2 volumes, Department of Earth and Atmospheric Sciences, St. Louis University, St. Louis, Missouri.

Hodgson, J. H. and R. S. Storey (1953). Tables extending Byerly's fault-plane techniques to earthquakes of any focal depth, *Bull. Seism. Soc. Am.* **43,** 49–61.

Hodgson, J. H. and J. F. J. Allen (1954a). Tables of extended distances for *PKP* and *PcP*, *Publ. Dom. Obs.* **26,** 329–348.

Hodgson, J. H. and J. F. J. Allen (1954b). Tables of extended distances for *PP* and *pP*, *Publ. Dom. Obs.* **26,** 351–362.

Hyndman, R. D., R. P. Riddihough, and R. Herzer (1979). The Nootka fault zone—A new plate boundary off western Canada, *Geophys. J. R. Astr. Soc.* **58,** 667–683.

Isacks, B., J. Oliver, and L. R. Sykes (1968). Seismology and the new global tectonics, *J. Geophys. Res.* **73,** 5855–5899.

Jeffreys, H. and K. E. Bullen (1958). *Seismological Tables*, British Association for the Advancement of Science, Gray Milne Trust, Office of the British Association, London, England, 50 pp.

Kanamori, H. and D. L. Anderson (1975). Theoretical basis of some empirical relations in seismology, *Bull. Seism. Soc. Am.* **65,** 1073–1095.

Lahr, J. C. (1984). HYPOELLIPSE/VAX: a computer program for determining local earthquake hypocentral parameters, magnitude, and first motion pattern, *U.S. Geol. Surv., Open-File Rept. 84-519*, 67 pp.

Milne, W. G. and K. A. Lucas (1961). Seismic activity in western Canada, 1955 to 1959 inclusive, *Publ. Dom. Obs.* **26,** 3–23.

Muller, J. E., B. E. B. Cameron, and K. E. Northcote (1980). Geology and mineral deposits of Nootka sound map—Area Vancouver Island, British Columbia, *Geol. Surv. Can. Paper 80-16*, Ottawa, Canada, 53 pp.

Page, R. (1968). Focal depths of aftershocks, *J. Geophys. Res.* **73,** 3897–3903.

Riddihough, R. P. (1977). A model for recent plate interactions off Canada's west coast, *Can. J. Earth Sci.* **14,** 384–396.

Riddihough, R. P. (1984). Recent movements of the Juan de Fuca Plate system, *J. Geophys. Res.* **89,** 6980–6994.

Rogers, G. C. (1976). The Vancouver Island earthquake of 5 July 1972, *Can. J. Earth Sci.* **13,** 92–101.

Rogers, G. C. (1979). Earthquake fault plane solutions near Vancouver Island, *Can. J. Earth Sci.* **16,** 523–531.

Rogers, G. C. (1983). Seismotectonics of British Columbia, *Ph.D. Thesis*, University of British Columbia, Vancouver, British Columbia, 247 pp.

Rogers, G. C. and H. S. Hasegawa (1978). A second look at the British Columbia earthquake of June 23, 1946, *Bull. Seism. Soc. Am.* **68,** 653–675.

Spence, G. D., R. M. Clowes, and R. M. Ellis (1985). Seismic structure across the active subduction zone of western Canada, *J. Geophys. Res.* **90,** 6754–6772.

Tobin, D. G. and L. R. Sykes (1968). Seismicity and tectonics of the northeast Pacific Ocean, *J. Geophys. Res.* **73,** 3821–3845.

Toppozada, T. R. (1975). Earthquake magnitude as a function of intensity data in California and western Nevada, *Bull. Seism. Soc. Am.* **65,** 1223–1238.

Tsai, Y.-B. and K. Aki (1970). Precise focal depth determination from amplitude spectra of surface waves, *J. Geophys. Res.* **75,** 5729–5743.

Vaněk, J., A. Zátopek, V. Kárnik, N. V. Kondorskaya, Y. V. Riznichenko, E. F. Savarensky, S. L.

Solov'yev, and N. V. Shebalin (1962). Standardization of magnitude scales, *Izv. Akad. Nauk SSSR, Ser. Geofiz.*, no. 2, 153–158 (English edition 108–111).

Veith, K. F. (1975). Refined hypocenters and accurate reliability estimates, *Bull. Seism. Soc. Am.* **65,** 1199–1222.

Weichert, D. H. and J. C. Newton (1970). Epicentre determination from first arrival times at Canadian stations, Seismology Series of the Earth Physics Branch, no. 59, Ottawa, Canada, 16 pp.

Wickens, A. J. and J. H. Hodgson (1967). Computer re-evaluation of earthquake mechanism solutions 1922–1962, *Publ. Dom. Obs.* **33,** 1–560.

Department of Geophysics and Astronomy
University of British Columbia
Vancouver, British Columbia,
Canada V6T 1W5 (J.F.C., R.M.E.)

Geological Survey of Canada
Pacific Geoscience Centre
P.O. Box 6000
Sidney, British Columbia,
Canada V8L 4B2 (G.C.R.)

Manuscript received 2 July 1987